Enhancing Cavity Quantum Electrodynamics via Antisqueezing: Synthetic Ultrastrong Coupling

C. Leroux,[1] L. C. G. Govia,[2] and A. A. Clerk[2]
[1]Department of Physics, McGill University, 3600 rue University, Montréal, Québec, Canada H3A 2T8
[2]Institute for Molecular Engineering, University of Chicago, 5640 South Ellis Avenue, Chicago, Illinois 60637, USA

(Received 28 September 2017; revised manuscript received 1 December 2017; published 2 March 2018)

We present and analyze a method where parametric (two-photon) driving of a cavity is used to exponentially enhance the light-matter coupling in a generic cavity QED setup, with time-dependent control. Our method allows one to enhance weak-coupling systems, such that they enter the strong coupling regime (where the coupling exceeds dissipative rates) and even the ultrastrong coupling regime (where the coupling is comparable to the cavity frequency). As an example, we show how the scheme allows one to use a weak-coupling system to adiabatically prepare the highly entangled ground state of the ultrastrong coupling system. The resulting state could be used for remote entanglement applications.

DOI: 10.1103/PhysRevLett.120.093602

Introduction.—Cavity QED (CQED), the interaction between a single two-level system (qubit) and a quantized mode of a cavity, is a ubiquitous platform [1] that has widespread utility, ranging from the study of fundamental physics [2], to the cutting edge of quantum information [3–5]. The most interesting regimes of CQED correspond to a qubit-cavity coupling that is strong enough to dominate dissipation rates. While historically this was very difficult to engineer [2], it has been achieved in several architectures, e.g. [6–12], though in many others it remains extremely challenging [13–16]. More challenging is reaching the so called ultrastrong coupling (USC) regime, where the coupling strength is comparable to the qubit or cavity frequency, or the deep-strong coupling (DSC) regime [17], where it exceeds the frequencies. Here, counter-rotating terms cannot be ignored, and the system is best described by the quantum Rabi model [18,19], which is known to exhibit a wide range of interesting phenomena, including strongly entangled and nonclassical eigenstates [20–24]. To date, only specially designed architectures have reached USC experimentally [25–29], though simulations of USC have also been considered [20,30,31].

In this Letter, we show how simple detuned parametric driving of a cavity can be used to dramatically enhance the effective qubit-cavity coupling in a generic CQED system. This can turn a weakly coupled system into a strongly coupled one, and even push one from strong coupling to USC or DSC. After describing the general idea, we show it enables the direct study of Rabi-model physics in a system whose bare coupling is far from the USC or DSC regimes. Further, the tunable nature of the coupling enhancement leads to new applications. We show how our approach allows one to leverage the entanglement of the DSC ground state to generate remote entanglement between the qubit and a traveling waveguide mode. This is a key ingredient in many quantum information protocols [32–35]. USC physics can also be exploited to realize powerful quantum computation and simulation protocols (see, e.g., [36–38]). Related approaches for coupling enhancement have been considered in the context of cavity optomechanics [39,40], a system with a markedly different kind of light-matter interaction.

Model.—We consider a qubit weakly coupled to a cavity, with the cavity subject to a two-photon (i.e. parametric) drive, see Fig. 1. Working in a frame rotating at half the parametric drive frequency $\omega_p/2$, the Hamiltonian is

$$\hat{H}(t) = \delta_c \hat{a}^\dagger \hat{a} + \frac{\delta_q}{2}\hat{\sigma}_z - \frac{\lambda(t)}{2}(\hat{a}^{\dagger 2} + \hat{a}^2) + g(\hat{a}^\dagger \hat{\sigma}_- + \hat{\sigma}_+ \hat{a}), \tag{1}$$

where $\hat{a}$ is the cavity annihilation operator and $\hat{\sigma}_\pm$ are qubit raising and lowering operators. $\lambda(t)$ is the time-dependent parametric drive amplitude, g is the qubit-cavity coupling strength, and $\delta_{c/q} = \omega_{c/q} - \omega_p/2$, are the cavity and qubit detunings (with $\omega_{c/q}$ being the cavity and qubit frequencies). The weak value of g implies that the qubit-cavity

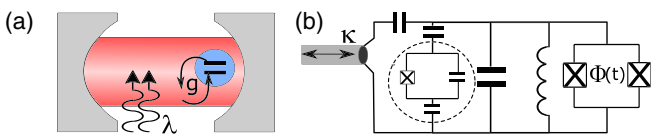

FIG. 1. (a) Schematic of the setup: a parametrically driven cavity (drive strength λ and drive frequency ω_p) is weakly coupled to a qubit with rate g. (b) A potential realization in circuit QED: a qubit coupled capacitively to a lumped-element cavity. A flux-pumped SQUID connected to the cavity implements the parametric drive, and the cavity couples to a transmission line with rate κ.

interaction is well-described by the excitation-conserving Jaynes-Cummings coupling written above. Note that a parametric drive can be implemented in many physical architectures. For example, in circuit QED, by modulating the flux through a cavity-embedded SQUID (see, e.g., [41]). In what follows, we exclusively consider detuned parametric drives with $|\delta_c| > \lambda$, which ensures that Eq. (1) is stable.

The instantaneous cavity-only part of $\hat{H}(t)$ can be diagonalized by the unitary $\hat{U}_S[r(t)] = \exp[r(t)(\hat{a}^2 - \hat{a}^{\dagger 2})/2]$, where the squeeze parameter $r(t)$ is defined via $\tanh 2r(t) = \lambda(t)/\delta_c$. The Hamiltonian in the time-dependent squeezed frame described by $\hat{U}_S[r(t)]$ is

$$\begin{aligned}\hat{H}^S(t) &\equiv \hat{U}_S[r(t)]\hat{H}\hat{U}_S^\dagger[r(t)] - i\dot{\hat{U}}_S\hat{U}_S^\dagger \\ &= \hat{H}_{\mathrm{Rabi}}(t) + \hat{H}_{\mathrm{Err}}(t) + \hat{H}_{\mathrm{DA}}(t), \end{aligned} \tag{2}$$

where

$$\begin{aligned}\hat{H}_{\mathrm{Rabi}}(t) &= \Omega_c[r(t)]\hat{a}^\dagger\hat{a} + \frac{\delta_q}{2}\hat{\sigma}_z + \frac{g}{2}e^{r(t)}(\hat{a}^\dagger + \hat{a})(\hat{\sigma}_+ + \hat{\sigma}_-), \\ \hat{H}_{\mathrm{Err}}(t) &= -\frac{g}{2}e^{-r(t)}(\hat{a}^\dagger - \hat{a})(\hat{\sigma}_+ - \hat{\sigma}_-), \\ \hat{H}_{\mathrm{DA}}(t) &= -\frac{i\dot{r}(t)}{2}(\hat{a}^{\dagger 2} - \hat{a}^2). \end{aligned} \tag{3}$$

The Hamiltonian $\hat{H}_{\mathrm{Rabi}}(t)$ has the form of the usual Rabi Hamiltonian, with enhanced coupling $\tilde{g} = ge^{r(t)}/2$ and effective cavity frequency $\Omega_c[r(t)] = \delta_c \mathrm{sech} 2r(t)$ (which decreases with increasing r). As $e^{r(t)}$ becomes arbitrarily large as we approach the instability threshold $\lambda = |\delta_c|$, the effective coupling in $\hat{H}_{\mathrm{Rabi}}$ can be orders of magnitude larger than the original coupling.

The remaining terms in Eqs. (3) describe undesired corrections to the ideal Rabi Hamiltonian. $\hat{H}_{\mathrm{Err}}(t)$ is explicitly suppressed by $e^{-r(t)}/2$, and it is negligible in the large amplification limit $e^{r(t)} \to \infty$ (as long as no external perturbation causes $(\hat{a} - \hat{a}^\dagger)$ to also become exponentially large in this limit). Note that cavity vacuum in the squeezed frame corresponds in the original lab frame to squeezed vacuum with squeeze parameter $r(t)$. The last correction term $\hat{H}_{\mathrm{DA}}(t)$ vanishes explicitly for a time-independent drive amplitude.

Thus, for large parametric drives, our system is *unitarily equivalent* to the Rabi-model Hamiltonian $\hat{H}_{\mathrm{Rabi}}(t)$ with an exponentially enhanced coupling strength. This enhancement is a consequence of the coherent parametric drive modifying the eigenstates of the cavity Hamiltonian: these are now squeezed photons, whose amplified fluctuations directly yield a larger interaction with the qubit. We stress that this enhancement is not equivalent to simply injecting squeezed light into the cavity (as this does not change the Hamiltonian). It is also distinct from the usual $\sqrt{n}$ enhancement associated with the Jaynes-Cumming interaction between a qubit and an n-photon Fock state, as in the squeezed frame, the interaction is enhanced for both small and large photon numbers.

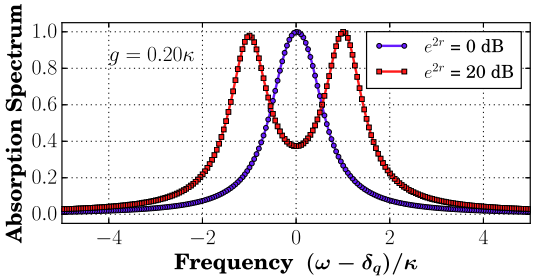

FIG. 2. The qubit absorption spectrum determined by a master equation simulation, for a resonant CQED system with $g = 0.2\kappa$, $\kappa = \gamma = 5 \times 10^{-4}\delta_c$. The blue (red) curve is for zero parametric drive (parametric drive corresponding to $e^{2r} = 20$ dB). The qubit frequency in the lab frame δ_q is chosen to maintain resonance with the cavity [i.e., $\delta_q = \Omega_c[r]$, cf. Eq. (2)]. For the red curve, the cavity is driven by squeezed vacuum, such that the system is in vacuum in the squeezed frame.

Weak to strong coupling.—The simplest application of our approach is to enhance the coupling in a weak-coupling CQED system (where g is much smaller than the cavity damping rate κ). Even if the resulting enhanced coupling $\tilde{g} < \kappa$, the increase could lead to dramatic enhancement of measurement sensitivity for spin or qubit detection, as the signal to noise ratio scales quadratically with $\tilde{g}$. This could be of particular utility in systems involving electronic or nuclear spins coupled to microwave cavities, where couplings are naturally weak [11–13,16]. The enhancement of a dispersive qubit measurement in this regime (where $\tilde{g} < \kappa$) can in some cases equivalently be understood from the perspective of amplification, see Ref. [42] for a full discussion.

Perhaps more interesting is the ability of our scheme to push a system from weak bare coupling ($g < \kappa$) to strong effective coupling, $\tilde{g} \gtrsim \kappa$, where we expect that the parametrically driven system will exhibit features of a true strong coupling CQED system. A hallmark of strong coupling is vacuum Rabi splitting (VRS) [2], where, e.g., the qubit absorption spectrum splits as a function of frequency (due to qubit-cavity hybridization). In Fig. 2, we show the qubit absorption spectrum (obtained from a master equation simulation [43]) as a function of frequency for a bare coupling $g = 0.20\kappa$, both with and without a parametric drive. As expected, the coupling enhancement due to the drive leads to a clear VRS. Note that to obtain a simple zero-temperature spectrum, we assume that the cavity is driven by squeezed vacuum noise in the lab frame, which corresponds to simple vacuum noise in the squeezed frame of Eq. (2). This ensures that the system starts in the ground state in the squeezed frame [43]. Injected squeezing is easily obtained in a variety of CQED setups (see, e.g., [44–47]).

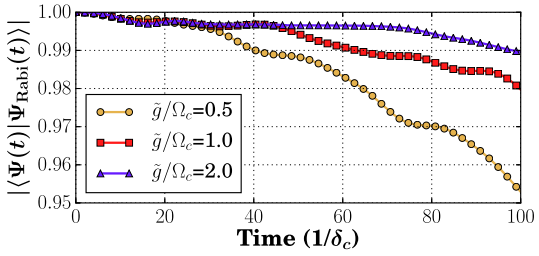

FIG. 3. *Simulation of a coupling quench*. The time-dependent overlap between the state $|\psi(t)\rangle$ obtained in our synthetic USC simulation and the state $|\psi_{\rm Rabi}(t)\rangle$ obtained in ideal Rabi-model evolution; the system starts in both cases in the weak-coupling ground state: cavity vacuum and $\hat{\sigma}_z$ ground state $|0,-z\rangle$. Different curves are for different values of dimensionless enhanced coupling $\tilde{g}/\Omega_c \equiv ge^r/2\Omega_c$. $\delta_q = 0.1\delta_c$ and $g = 0.05\delta_c$. Dissipation is neglected.

Strong coupling in CQED enables a number of applications, ranging from nonlinear quantum optics at the two-photon level to single-atom lasing [9]. Parametric driving makes these accessible even in systems with weak bare coupling.

Dynamical simulation of a USC or DSC quench.—Parametric driving can be pushed further, enhancing a weak or strong coupling CQED system into the USC or DSC regimes. In Fig. 3, we show that our approach allows a faithful realization of the USC or DSC regimes by comparing the dynamical evolution of the parametrically driven system [including all terms in Eq. (2)] against a simulation of just the ideal Rabi Hamiltonian $\hat{H}_{\rm Rabi}$. We start the system in the $g = 0$ ground state of Eq. (2), and thus are simulating a quench-type protocol where the (ultrastrong or deep-strong) coupling is suddenly turned on. Figure 3 plots the time-dependent fidelity between the simulated state and the ideal Rabi-model state, for several values of parametric drive strength. The parametrically driven system faithfully reproduces the ideal Rabi-model evolution over long time scales. The fidelity is even better for larger coupling enhancements, as the larger the squeezing, the more the suppression of the unwanted terms in $\hat{H}_{\rm Err}$ [cf. Eqs. (3)].

Adiabatic preparation of entangled USC or DSC ground states.—In contrast to the above quench protocol, we can start with the trivial ground state of a weakly coupled CQED system [i.e., ground state of Eq. (1) for $\lambda(t) = 0$], and then adiabatically prepare the ground state of the ultrastrong or deep-strong coupling Rabi model by slowly ramping up the parametric drive amplitude. Further, once the desired state is achieved, the parametric drive can be turned off, returning the system to weak-coupling dynamics.

The ability to prepare USC or DSC ground states and then return to weak coupling allows a number of useful protocols. After preparation, one could turn off the coupling and allow the cavity state to leak into a waveguide or transmission line, implying that any cavity-qubit entanglement is now qubit-propagating photon entanglement; this enables remote entanglement protocols. Alternatively, as the protocol ends with the system in a weak coupling regime, the cavity state can be directly probed using standard weak-coupling techniques, for example by using the qubit [5,48–51]. This addresses the long-standing issue of how to observe the nontrivial aspects of the ground state of the quantum Rabi model.

While this approach can prepare the ground state of the Rabi Hamiltonian $\hat{H}_{\rm Rabi}(t)$ in any parameter regime, we focus on the DSC case $\delta_q = 0$, $\tilde{g} \gtrsim \Omega_c$, where the ground state has the form of an entangled cat state:

$$|\Psi_{\rm Target}(t)\rangle = \frac{|\alpha(t)\rangle|+x\rangle - |-\alpha(t)\rangle|-x\rangle}{\sqrt{2}}. \tag{4}$$

Here, $|\alpha\rangle$ denotes a coherent state in the cavity, and $|\pm x\rangle$ denote $\hat{\sigma}_x$ eigenstates; the displacement $\alpha \propto \tilde{g}$ (see Supplemental Material for the full expression [43]). Note that as this is the ground state in the squeezed frame, in the original lab frame the state will correspond to the qubit being entangled with squeezed, displaced cavity pointer states.

As discussed above, preparing this state and then turning off the parametric drive allows one to create a nontrivial entangled state where the qubit is entangled with a propagating (squeezed, displaced) wave packet. Unlike more standard approaches (e.g., [52]), this is accomplished without any controls or drives applied directly to the qubit. In the following, we focus on the adiabatic preparation of a strongly entangled local cavity-qubit state using our scheme, as how to use such a state to generate remote entanglement has been studied extensively elsewhere (see, e.g., [34,53–56]). In the Supplemental Material, we outline the transfer of the cavity state into a waveguide, and we briefly comment on the effects of internal loss [43].

To consider the robustness of our approach, we simulate adiabatic state preparation in the presence of cavity and qubit dissipation. These are treated via a standard Lindblad master equation, which in the original lab frame takes the form:

$$\dot{\hat{\rho}} = i[\hat{\rho}, \hat{H}(t)] + \gamma\mathcal{D}[\hat{\sigma}_-]\hat{\rho} + \kappa\mathcal{D}[\hat{a}]\hat{\rho}, \tag{5}$$

where $\mathcal{D}[\hat{x}]\hat{\rho} = \hat{x}\,\hat{\rho}\,\hat{x}^\dagger - \frac{1}{2}\{\hat{x}^\dagger\hat{x}, \hat{\rho}\}$, κ is the cavity damping rate, γ is the intrinsic qubit decay rate, and we have assumed zero temperature environments. Note that the simple form of this master equation is justified by the fact that we have a driven system with a large drive frequency ω_p (see Supplemental Material [43]); as a result, complications associated with strong-coupling master equations [57] do not apply.

We parametrize the time-dependent parametric drive amplitude $\lambda(t)$ via $\tanh 2r(t) = \lambda(t)/\delta_c$ and $r(t) = r_{\rm max}\tanh(t/2\tau)$, where τ sets the effective protocol speed,

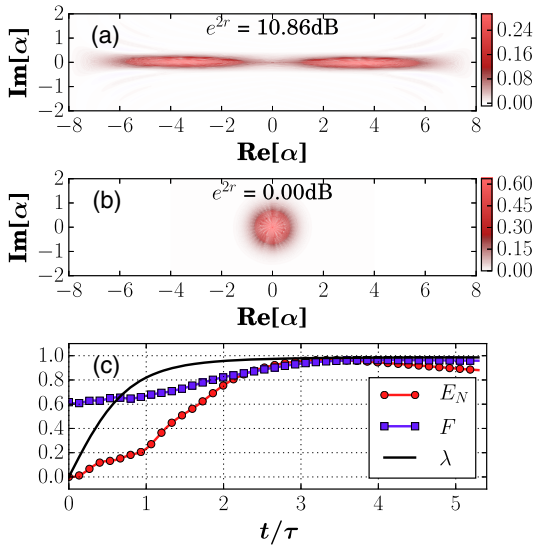

FIG. 4. *Adiabatic preparation of an entangled deep-strong coupling ground state*. (a) A CQED system with $g=0.1\delta_c$, $\delta_q=0$ is initially prepared in the weak coupling ground state $|\Psi^S(0)\rangle = |0\rangle|-z\rangle$. The parametric drive is turned on adiabatically (see main text) at a rate of $1/\tau = 0.1\delta_c$, to a final value corresponding to a parametric gain $e^{2r_{\max}} = 10.86$ dB (i.e., $r_{\max} = 1.25$). The Wigner function of the final cavity state is shown; the structure corresponds to the expected entangled Rabi model ground state written in Eq. (4). (b) The final state after the same evolution period but with no parametric drive and coupling enhancement; the Wigner function corresponds to the trivial weak coupling ground state. (c) The time-evolution of the logarithmic negativity $E_N(t)$, the fidelity $F(t)$ [cf. Eq. (6)], and the parametric drive amplitude $\lambda(t)$ for a parametric gain of 10.86 dB. E_N approaches its maximum value of 1. For all plots, $\gamma=5\times10^{-5}\delta_c$, $\kappa = 10^{-4}\delta_c$, and $t_f \simeq 5\tau$. For an experimentally realistic detuning of $\delta_c = 1$ GHz, the parameters correspond to $g = 100$ MHz, a cavity decay rate $\kappa = 100$ kHz, and a qubit lifetime $1/\gamma = 20$ μs.

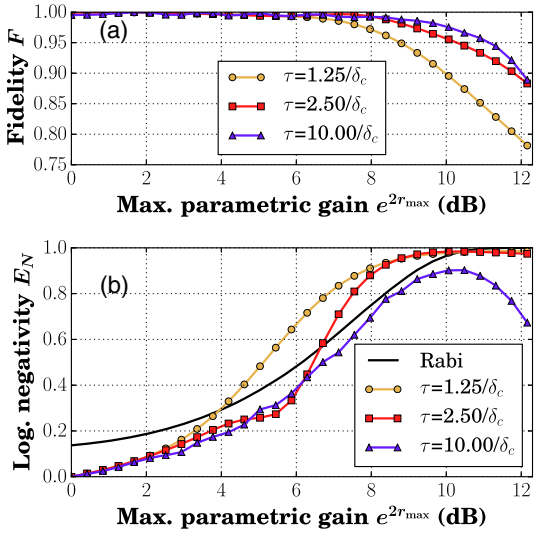

FIG. 5. (a) The final state fidelity $F(t_f)$ [cf. Eq. (6)] and (b) entanglement (measured via the logarithmic negativity E_N) as a function of the final parametric gain $e^{2r_{\max}}$; different curves are for different values of the protocol speed parameter τ. The total time of each simulation is $t_f \simeq 5\tau$. The black curve in (b) is E_N in the ground state of the ideal Rabi-model Hamiltonian [cf. $\hat{H}_{\rm Rabi}$ in Eq. (2)] with equivalent parameters: coupling $ge^{r_{\max}}/2$, cavity frequency $\delta_c \mathrm{sech} 2r_{\max}$ and qubit frequency δ_q. Other simulation parameters are the same as in Fig. 4.

and $r_{\max}$ is the final maximum value of the squeeze parameter. The evolution runs from $t = 0$ to $t = t_f \gg \tau$. We quantify the protocol's success using the fidelity $F(t)$ between the dynamically generated state and the desired target state of Eq. (4),

$$F(t) = \sqrt{\langle \Psi_{\rm Target}(t_f)|\hat{\rho}^S(t)|\Psi_{\rm Target}(t_f)\rangle}, \qquad (6)$$

where $\hat{\rho}^S(t)$ denotes the system density matrix in the squeezed frame. Achieving a good fidelity involves picking a value of τ that is large enough to ensure adiabaticity but not so large that dissipative effects corrupt the evolution.

Figure 4 summarizes the results of a simulation of our scheme for a system with $g = 0.1\delta_c$, starting in the zero-coupling ground state $|0,-z\rangle$, for a protocol time scale $\tau = 10\delta_c^{-1}$. Panel (b) shows the Wigner function of the cavity state obtained if the parametric drive is off during this evolution time: it corresponds to vacuum. Panel (a) shows instead the Wigner function obtained when the parametric drive is ramped such that $e^{2r_{\max}} = 11$ dB. One clearly sees the double-blob structure associated with the target state in Eq. (4), and Fig. 4(c) shows that one indeed has good fidelity with this state, with the expected near-maximal amount of qubit-cavity entanglement (characterized by the logarithmic negativity E_N).

It is also interesting to consider the performance of the adiabatic state preparation as a function of the parametric gain $e^{2r_{\max}}$. Figure 5(a) shows the behavior of the fidelity at the end of the protocol as a function of the gain; different curves are for different ramp rates $1/\tau$. The fidelity generically drops off at high amplification factors, which is due to increased nonadiabatic errors [$\hat{H}_{\rm DA}$ in Eqs. (3)], and dissipation. In the lab frame, the cavity is driven by vacuum noise associated with the loss κ. However, in the squeezed frame used to write Eq. (2), this noise appears squeezed. This unwanted squeezing is oriented along the $i(\hat{a}^\dagger - \hat{a})$ quadrature, such that its fluctuations enhance the spurious (exponential damped) $\hat{H}_{\rm Err}$ term in Eq. (2), and it also has effects akin to heating; this all leads to errors in the adiabatic protocol. Figure 5(b) shows the corresponding behavior of the qubit-cavity entanglement (measured by the logarithmic negativity E_N). Surprisingly, the entanglement does not mirror the behavior of the fidelity, and for rapid protocols, it can be larger than in the ideal target state. Optimizing our scheme for rapid entanglement generation could be an interesting focus of future study.

Conclusion.—We have analyzed how parametric driving of a cavity can enable a strong coupling enhancement in

CQED, even letting a weak coupling system reach the regime of ultrastrong or deep-strong coupling. The time-dependent control of the enhancement allows a variety of protocols, including the adiabatic preparation of highly entangled states. Our scheme is well-suited for contemporary circuit QED technology, where strong parametric interactions [41,58] and high coherence times [59,60] are commonplace. Microwave resonators with strong parametric interactions can also be coupled to nitrogen-vacancy centers [14], Rydberg atoms [61], or quantum dots [11,12], and our scheme can be used for enhanced CQED here as well.

Our scheme is not limited to microwaves. All requirements have been independently implemented at optical frequencies, though to our knowledge they have not been combined in a single experiment. Combining a pumped χ^2 nonlinear resonator [62–64] (perhaps in a photonic crystal cavity) with a quantum dot [65] or atomic emitter [66] is one promising pathway for realizing our scheme at optical frequencies. Mechanical systems coupled to NV center [67] or quantum dot (see, e.g., [68,69]) qubits are another possible application. Our scheme can be generalized to realize regimes of ultrastrong coupling in lattices of CQED cavities [70] by introducing local parametric driving at each site, and it can be applied to generate multiqubit entanglement in a multiqubit, single mode setup [71].

This work was supported by NSERC and the AFOSR MURI FA9550-15-1-0029.

[1] H. Walther, B. T. H. Varcoe, B.-G. Englert, and T. Becker, Rep. Prog. Phys. **69**, 1325 (2006).

[2] S. Haroche and J.-M. Raimond, *Exploring the Quantum: Atoms, Cavities, and Photons* (Oxford University Press, Oxford, 2006) p. 616.

[3] D. C. McKay, R. Naik, P. Reinhold, L. S. Bishop, and D. I. Schuster, Phys. Rev. Lett. **114**, 080501 (2015).

[4] P. J. J. O'Malley, R. Babbush, I. D. Kivlichan, J. Romero, J. R. McClean, R. Barends, J. Kelly, P. Roushan, A. Tranter, N. Ding, B. Campbell, Y. Chen, Z. Chen, B. Chiaro, A. Dunsworth, A. G. Fowler, E. Jeffrey, E. Lucero, A. Megrant, J. Y. Mutus *et al.*, Phys. Rev. X **6**, 031007 (2016).

[5] C. Wang, Y. Y. Gao, P. Reinhold, R. W. Heeres, N. Ofek, K. Chou, C. Axline, M. Reagor, J. Blumoff, K. M. Sliwa, L. Frunzio, S. M. Girvin, L. Jiang, M. Mirrahimi, M. H. Devoret, and R. J. Schoelkopf, Science **352**, 1087 (2016).

[6] M. Brune, J. M. Raimond, P. Goy, L. Davidovich, and S. Haroche, Phys. Rev. Lett. **59**, 1899 (1987).

[7] R. J. Thompson, G. Rempe, and H. J. Kimble, Phys. Rev. Lett. **68**, 1132 (1992).

[8] A. Wallraff, D. I. Schuster, A. Blais, L. Frunzio, R. S. Huang, J. Majer, S. Kumar, S. M. Girvin, and R. J. Schoelkopf, Nature (London) **431**, 162 (2004).

[9] G. Khitrova, H. M. Gibbs, M. Kira, S. W. Koch, and A. Scherer, Nat. Phys. **2**, 81 (2006).

[10] J. J. Viennot, M. C. Dartiailh, A. Cottet, and T. Kontos, Science **349**, 408 (2015).

[11] X. Mi, J. V. Cady, D. M. Zajac, P. W. Deelman, and J. R. Petta, Science **355**, 156 (2017).

[12] A. Stockklauser, P. Scarlino, J. V. Koski, S. Gasparinetti, C. K. Andersen, C. Reichl, W. Wegscheider, T. Ihn, K. Ensslin, and A. Wallraff, Phys. Rev. X **7**, 011030 (2017).

[13] D. I. Schuster, A. P. Sears, E. Ginossar, L. DiCarlo, L. Frunzio, J. J. L. Morton, H. Wu, G. A. D. Briggs, B. B. Buckley, D. D. Awschalom, and R. J. Schoelkopf, Phys. Rev. Lett. **105**, 140501 (2010).

[14] Y. Kubo, F. R. Ong, P. Bertet, D. Vion, V. Jacques, D. Zheng, A. Dréau, J.-F. Roch, A. Auffeves, F. Jelezko, J. Wrachtrup, M. F. Barthe, P. Bergonzo, and D. Esteve, Phys. Rev. Lett. **105**, 140502 (2010).

[15] K. D. Petersson, L. W. McFaul, M. D. Schroer, M. Jung, J. M. Taylor, A. A. Houck, and J. R. Petta, Nature (London) **490**, 380 (2012).

[16] A. Bienfait, J. J. Pla, Y. Kubo, M. Stern, X. Zhou, C. C. Lo, C. D. Weis, T. Schenkel, M. L. W. Thewalt, D. Vion, D. Esteve, B. Julsgaard, K. Mølmer, J. J. L. Morton, and P. Bertet, Nat. Nanotechnol. **11**, 253 (2016).

[17] J. Casanova, G. Romero, I. Lizuain, J. J. García-Ripoll, and E. Solano, Phys. Rev. Lett. **105**, 263603 (2010).

[18] I. I. Rabi, Phys. Rev. **49**, 324 (1936).

[19] I. I. Rabi, Phys. Rev. **51**, 652 (1937).

[20] D. Ballester, G. Romero, J. J. García-Ripoll, F. Deppe, and E. Solano, Phys. Rev. X **2**, 021007 (2012).

[21] S. Ashhab and F. Nori, Phys. Rev. A **81**, 042311 (2010).

[22] D. Braak, Q.-H. Chen, M. T. Batchelor, and E. Solano, J. Phys. A **49**, 300301 (2016).

[23] N. Gheeraert, S. Bera, and S. Florens, New J. Phys. **19**, 023036 (2017).

[24] C. Leroux, L. C. G. Govia, and A. A. Clerk, Phys. Rev. A **96**, 043834 (2017).

[25] A. A. Anappara, S. De Liberato, A. Tredicucci, C. Ciuti, G. Biasiol, L. Sorba, and F. Beltram, Phys. Rev. B **79**, 201303 (2009).

[26] G. Gunter, A. A. Anappara, J. Hees, A. Sell, G. Biasiol, L. Sorba, S. De Liberato, C. Ciuti, A. Tredicucci, A. Leitenstorfer, and R. Huber, Nature (London) **458**, 178 (2009).

[27] T. Niemczyk, F. Deppe, H. Huebl, E. P. Menzel, F. Hocke, M. J. Schwarz, J. J. Garcia-Ripoll, D. Zueco, T. Hummer, E. Solano, A. Marx, and R. Gross, Nat. Phys. **6**, 772 (2010).

[28] P. Forn-Díaz, J. Lisenfeld, D. Marcos, J. J. García-Ripoll, E. Solano, C. J. P. M. Harmans, and J. E. Mooij, Phys. Rev. Lett. **105**, 237001 (2010).

[29] F. Yoshihara, T. Fuse, S. Ashhab, K. Kakuyanagi, S. Saito, and K. Semba, Nat. Phys. **13**, 44 (2017).

[30] A. Mezzacapo, U. Las Heras, J. S. Pedernales, L. DiCarlo, E. Solano, and L. Lamata, Sci. Rep. **4**, 7482 (2014).

[31] N. K. Langford, R. Sagastizabal, M. Kounalakis, C. Dickel, A. Bruno, F. Luthi, D. J. Thoen, A. Endo, and L. DiCarlo, Nat. Commun. **8**, 1715 (2017).

[32] C. H. Bennett, G. Brassard, C. Crépeau, R. Jozsa, A. Peres, and W. K. Wootters, Phys. Rev. Lett. **70**, 1895 (1993).

[33] D. Gottesman and I. L. Chuang, Nature (London) **402**, 390 (1999).

[34] N. Sangouard, C. Simon, H. de Riedmatten, and N. Gisin, Rev. Mod. Phys. **83**, 33 (2011).

[35] H. J. Kimble, Nature (London) **453**, 1023 (2008).

[36] P. Nataf and C. Ciuti, Phys. Rev. Lett. **107**, 190402 (2011).
[37] G. Romero, D. Ballester, Y. M. Wang, V. Scarani, and E. Solano, Phys. Rev. Lett. **108**, 120501 (2012).
[38] Y. Wang, J. Zhang, C. Wu, J. Q. You, and G. Romero, Phys. Rev. A **94**, 012328 (2016).
[39] X.-Y. Lü, Y. Wu, J. R. Johansson, H. Jing, J. Zhang, and F. Nori, Phys. Rev. Lett. **114**, 093602 (2015).
[40] M.-A. Lemonde, N. Didier, and A. A. Clerk, Nat. Commun. **7**, 11338 (2016).
[41] T. Yamamoto, K. Inomata, M. Watanabe, K. Matsuba, T. Miyazaki, W. D. Oliver, Y. Nakamura, and J. S. Tsai, Appl. Phys. Lett. **93**, 042510 (2008).
[42] B. Levitan, Master's thesis, McGill University (2016).
[43] See the Supplemental Material at http://link.aps.org/supplemental/10.1103/PhysRevLett.120.093602 for further details of our calculations and simulations.
[44] S. L. Braunstein and P. van Loock, Rev. Mod. Phys. **77**, 513 (2005).
[45] A. I. Lvovsky, *Photonics Volume 1: Fundamentals of Photonics and Physics* (Wiley, West Sussex, 2015) pp. 121–164.
[46] K. G. Fedorov, L. Zhong, S. Pogorzalek, P. Eder, M. Fischer, J. Goetz, E. Xie, F. Wulschner, K. Inomata, T. Yamamoto, Y. Nakamura, R. Di Candia, U. Las Heras, M. Sanz, E. Solano, E. P. Menzel, F. Deppe, A. Marx, and R. Gross, Phys. Rev. Lett. **117**, 020502 (2016).
[47] D. M. Toyli, A. W. Eddins, S. Boutin, S. Puri, D. Hover, V. Bolkhovsky, W. D. Oliver, A. Blais, and I. Siddiqi, Phys. Rev. X **6**, 031004 (2016).
[48] P. Bertet, A. Auffeves, P. Maioli, S. Osnaghi, T. Meunier, M. Brune, J. M. Raimond, and S. Haroche, Phys. Rev. Lett. **89**, 200402 (2002).
[49] M. Hofheinz, H. Wang, M. Ansmann, R. C. Bialczak, E. Lucero, M. Neeley, A. D. O'Connell, D. Sank, J. Wenner, J. M. Martinis, and A. N. Cleland, Nature (London) **459**, 546 (2009).
[50] B. Vlastakis, G. Kirchmair, Z. Leghtas, S. E. Nigg, L. Frunzio, S. M. Girvin, M. Mirrahimi, M. H. Devoret, and R. J. Schoelkopf, Science **342**, 607 (2013).
[51] E. Flurin, V. V. Ramasesh, S. Hacohen-Gourgy, L. S. Martin, N. Y. Yao, and I. Siddiqi, Phys. Rev. X **7**, 031023 (2017).
[52] B. Vlastakis, A. Petrenko, N. Ofek, L. Sun, Z. Leghtas, K. Sliwa, Y. Liu, M. Hatridge, J. Blumoff, L. Frunzio, M. Mirrahimi, L. Jiang, M. H. Devoret, and R. J. Schoelkopf, Nat. Commun. **6**, 8970 (2015).
[53] J. I. Cirac, P. Zoller, H. J. Kimble, and H. Mabuchi, Phys. Rev. Lett. **78**, 3221 (1997).
[54] Y. Yin, Y. Chen, D. Sank, P. J. J. O'Malley, T. C. White, R. Barends, J. Kelly, E. Lucero, M. Mariantoni, A. Megrant, C. Neill, A. Vainsencher, J. Wenner, A. N. Korotkov, A. N. Cleland, and J. M. Martinis, Phys. Rev. Lett. **110**, 107001 (2013).
[55] M. Pechal, L. Huthmacher, C. Eichler, S. Zeytinoğlu, A. A. Abdumalikov, S. Berger, A. Wallraff, and S. Filipp, Phys. Rev. X **4**, 041010 (2014).
[56] W. Pfaff, C. J. Axline, L. D. Burkhart, U. Vool, P. Reinhold, L. Frunzio, L. Jiang, M. H. Devoret, and R. J. Schoelkopf, Nat. Phys. **13**, 882 (2017).
[57] F. Beaudoin, J. M. Gambetta, and A. Blais, Phys. Rev. A **84**, 043832 (2011).
[58] I. Siddiqi, R. Vijay, F. Pierre, C. M. Wilson, M. Metcalfe, C. Rigetti, L. Frunzio, and M. H. Devoret, Phys. Rev. Lett. **93**, 207002 (2004).
[59] Y. Chen, C. Neill, P. Roushan, N. Leung, M. Fang, R. Barends, J. Kelly, B. Campbell, Z. Chen, B. Chiaro, A. Dunsworth, E. Jeffrey, A. Megrant, J. Y. Mutus, P. J. J. O'Malley, C. M. Quintana, D. Sank, A. Vainsencher, J. Wenner, T. C. White *et al.*, Phys. Rev. Lett. **113**, 220502 (2014).
[60] M. Reagor, W. Pfaff, C. Axline, R. W. Heeres, N. Ofek, K. Sliwa, E. Holland, C. Wang, J. Blumoff, K. Chou, M. J. Hatridge, L. Frunzio, M. H. Devoret, L. Jiang, and R. J. Schoelkopf, Phys. Rev. B **94**, 014506 (2016).
[61] J. D. Pritchard, J. A. Isaacs, M. A. Beck, R. McDermott, and M. Saffman, Phys. Rev. A **89**, 010301 (2014).
[62] W. T. M. Irvine, K. Hennessy, and D. Bouwmeester, Phys. Rev. Lett. **96**, 057405 (2006).
[63] J. U. Fürst, D. V. Strekalov, D. Elser, A. Aiello, U. L. Andersen, C. Marquardt, and G. Leuchs, Phys. Rev. Lett. **106**, 113901 (2011).
[64] M. Förtsch, J. U. Fürst, C. Wittmann, D. Strekalov, A. Aiello, M. V. Chekhova, C. Silberhorn, G. Leuchs, and C. Marquardt, Nat. Commun. **4**, 1818 (2013).
[65] A. Imamoğlu, S. Fält, J. Dreiser, G. Fernandez, M. Atatüre, K. Hennessy, A. Badolato, and D. Gerace, J. Appl. Phys. **101**, 081602 (2007).
[66] T. G. Tiecke, J. D. Thompson, N. P. de Leon, L. R. Liu, V. Vuletić, and M. D. Lukin, Nature (London) **508**, 241 (2014).
[67] D. Lee, K. W. Lee, J. V. Cady, P. Ovartchaiyapong, and A. C. B. Jayich, J. Opt. **19**, 033001 (2017).
[68] S. D. Bennett, L. Cockins, Y. Miyahara, P. Grütter, and A. A. Clerk, Phys. Rev. Lett. **104**, 017203 (2010).
[69] I. Yeo, P.-L. de Assis, A. Gloppe, E. Dupont-Ferrier, P. Verlot, N. S. Malik, E. Dupuy, J. Claudon, J.-M. Gérard, A. Auffèves, G. Nogues, S. Seidelin, J.-P. Poizat, O. Arcizet, and M. Richard, Nat. Nanotechnol. **9**, 106 (2013).
[70] A. A. Houck, H. E. Türeci, and J. Koch, Nat. Phys. **8**, 292 (2012).
[71] F. Armata, G. Calajo, T. Jaako, M. S. Kim, and P. Rabl, Phys. Rev. Lett. **119**, 183602 (2017).